Materials Today: Proceedings 90 (2023) 128–132

Contents lists available at ScienceDirect

Materials Today: Proceedings

journal homepage: www.elsevier.com/locate/matpr

# Effect of thickness on the EMI shielding effectiveness of epoxy composites with cobalt ferrite and graphene

Manobalan S. [a], Suryasarathi Bose [b], Sumangala T.P. [a,*]

[a] Department of Physics, School of Advanced Sciences, Vellore Institute of Technology, Vellore 632014, India
[b] Department of Materials Engineering, Indian Institute of Science, C.V. Raman Avenue, Bangalore 560012, India

ARTICLE INFO

*Article history:*
Available online 15 May 2023

*Keywords:*
EMI Shielding
Polymer composites
Absorption loss

ABSTRACT

The study investigates the impact of thickness on the electromagnetic interference (EMI) shielding effectiveness (SE) of Cobalt ferrite/ Graphene/ Epoxy (GrEpCoF) composite samples. Samples were prepared using a simple casting method. Cobalt ferrite was synthesized using hydrothermal method. The XRD of pure epoxy, graphene and cobalt ferrite is obtained. Microstructure of pristine epoxy and GrEp sample was studied using SEM. Further GrEpCoF with varying thickness was prepared. The impact of thickness on both the electric as well as the magnetic loss was studied for two bands, viz. X-band (8.2–12.4 GHZ) and Ku band (12.4–18) GHz. In addition, the EMI SE is also explored for these samples.

Selection and peer-review under responsibility of the scientific committee of the International Conference on Future Technologies in Manufacturing, Automation, Design & Energy.

## 1. Introduction

Electromagnetic interference (EMI) and radiation pollution brought on by electromagnetic waves are becoming significant issues as a result of quick developments in the fifth-generation (5G) communication technology especially in areas such as consumer electronics, intelligent systems, and data protection. Transmission of electromagnetic waves puts human health at extreme risk and raises issues with electronic communication devices and their delicate components [1,3]. EMI shielding composites made of polymers-based composites (PBC) have developed into a heavily researched area due to their benefits of being lightweight, having great corrosion resistance, providing constant EMI shielding performance, and displaying outstanding mechanical features [2,4–7]. A material's superior electrical insulating ability, however, cannot actually address a material's higher EMI shielding capacity [8].

Electromagnetic shielding composites made of individual conductive particles or magnetic particles frequently fail to fulfil the criteria of bandwidth, low weight, compact size, and good performance for EMI shielding materials. To achieve their exceptional EMI shielding properties, conductive and magnetic additives are typically used in PBC.

Epoxy resins, polyvinylidene fluoride (PVDF), polyaniline, polyimide (PI), polyethylene (PE), and polypropylene (PP), are a few examples of frequently used polymer matrix materials [9–11]. Ferrites are often used as magnetic materials in the field of EMI shielding because they are affordable, easy to produce, and have higher values of saturation magnetisation (180 – 420 G). There are different ferrites used in the application of EMI shielding including nickel ferrite [11], cobalt ferrite [12,13] and manganese-zinc ferrite [14,15].We report the investigation of the impact of sample thickness on the dielectric loss, magnetic loss and total EMI SE in both X-band and Ku-band of composites with graphene (Gr) and Cobalt ferrite (CoF) as filler in Epoxy (Ep) matrix.

## 2. Experimental section

### 2.1. Materials

A few layers Graphene (>99% purity) with surface area 200 – 700 $m^2/g$ was procured from Ad Nano, India. For the matrix, the Epoxy resin (LY556) and Hardener (HY951) were obtained from Go Green Products, India. The precursors for the synthesis of cobalt ferrite viz. Ferric chloride (Sigma Aldrich), cobalt chloride hexahydrate (Sigma Aldrich), and Sodium Hydroxide (Merck India) were used without additional purification.

* Corresponding author.
*E-mail addresses:* suma.tp85@gmail.com, sumangala.tp@vit.ac.in (S. T.P.).

https://doi.org/10.1016/j.matpr.2023.05.078

Selection and peer-review under responsibility of the scientific committee of the International Conference on Future Technologies in Manufacturing, Automation, Design & Energy.

### 2.2. Cobalt ferrite synthesis via. Hydrothermal method

The hydrothermal approach was used to prepare cobalt ferrite ($CoFe_2O_4$, CoF) nanoparticles (NPs). 1.0 M ferric chloride ($FeCl_3$) and 0.5 M Cobalt chloride ($CoCl_3$) were typically mixed in DI water at a temperature of 80 °C utilising a hot plate with a magnetic stirrer attachment. The precursors were dissolved in DI water, and a moderate amount of NaOH solution was added gradually until the pH of the combination reached 10. Further, the resultant solution was transferred into autoclave at a temperature 180 °C for 8 h. The solution was then centrifuged and repeatedly rinsed in deionized water. Subsequently, this was dried overnight at 90 °C . The powder that resulted from it was calcined at 300 °C for 2 h to produce CoF NPs. Fig. 1 (a) illustrates the steps required to prepare CoF.

### 2.3. Preparation of composites

For the preparation of composites, a 10: 1 ratio of epoxy and hardener was employed. During composite preparations, 1.5 wt% of graphene and the necessary amounts of epoxy were physically mixed for 10 min. Graphene/Epoxy/Cobalt nanocomposite were produced by combining 5 wt% of Cobalt ferrite (CoF). For an additional 15 min, this was mixed. Hardener was included after this step. The mixture was stirred homogeneously to initiate the curing process. Then the colloidal solution was transferred into suitable silicon rubber mould with desired shape for further characterization. The thickness of the composite sample was varied by using silicon rubber mould of varying thickness (ranging from 2 mm to 7.5 mm). Fig. 1(a) also provides a visual representation of the manufacturing of composites.

The XRD spectrum was captured using a Bruker (Germany) X-ray diffractometer with Cu-Kα radiation of wavelength 1.5406 Å. Field emission scanning electron microscope, Thermo Fisher FEI QUANTA 250 FEG (USA) (FE-SEM), Keysight N 9911a, vector network analyser and Novocontrol, Germany was employed for microstructural, EMI Shielding effectiveness and permeability, permittivity measurements respectively.

## 3. Results and discussions

### 3.1. Structural characterisation

Fig. 1(b) displays the XRD pattern for the CoF, Gr, and GrEp composite. XRD confirms the presence of single-phase spinel $CoFe_2O_4$ (JCPDS card no. 22–1086). A peak at 25° may be seen in the XRD pattern of pure graphene. The pattern for sample EpGr exhibits two diffused peaks with centres at 17.5° and 45°. This could be attributed to the amorphous nature of epoxy.

### 3.2. Morphological characterisation

SEM was used to examine the structure of pure epoxy and the distribution of graphene within the epoxy matrix. There were smooth, continuous layers of epoxy visible in the cross-sectional SEM of pristine epoxy (Fig. 2 (a)). However, in contrary to the smooth surface of pristine epoxy, a crumbled surface was visible in EpGr composite. The sheet like morphology of graphene and their uniform dispersion was visible from Fig. 2(b). The graphene sheets formed interconnecting network in epoxy matrix.

### 3.3. Dielectric loss and magnetic loss

Fig. 3(a-d) displayed the magnetic loss and the dielectric loss for the bands X, Ku. The maximum dielectric loss of −26 (negative direction) is achieved in the X-band spectrum (8.2–12.4 GHz) for the sample, GrEpCoF, with 7 mm thickness (Fig. 3 (a)). Except for the composite with the thickness of 7 mm, remaining samples showed very less dielctric loss. The dielectric loss are negligible in Ku-band as clearly seen from Fig. 3(b).

The maximum magnetic loss of upto −2 (negative direction) was observed with the 7.5 mm composite (Fig. 3(c)). Other samplers exhibited very low values of magnetic loss. The magnetic loss are negligible in Ku band as well for composites of various thickness (Fig. 3(d)).

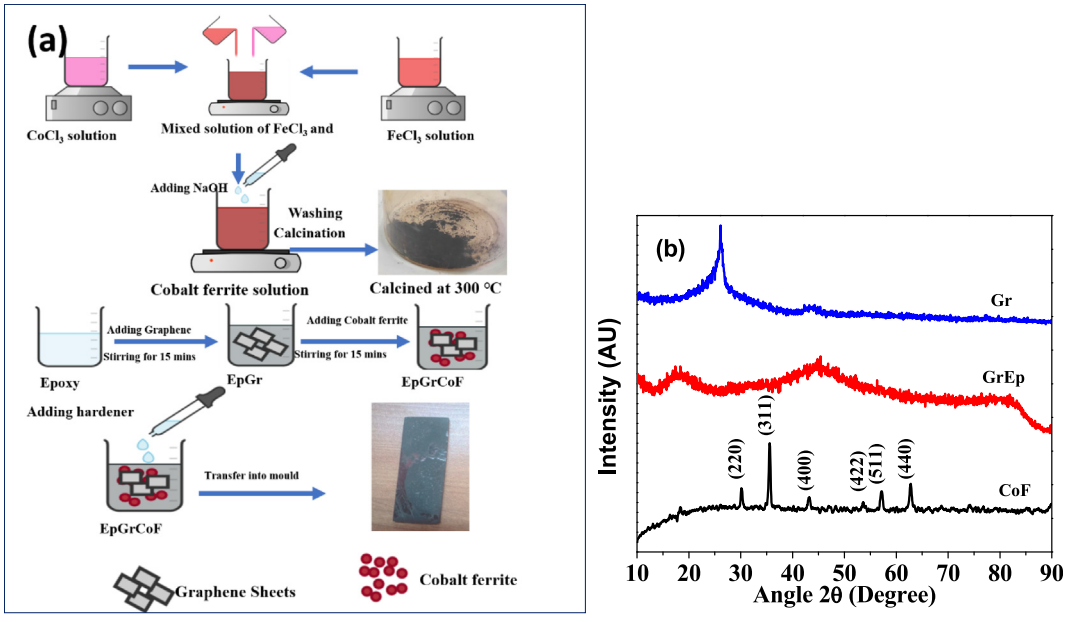


**Fig. 1.** (a) Schematic representation of the steps involved in sample preparation, (b) XRD pattern of CoF, GrEp and Gr samples.

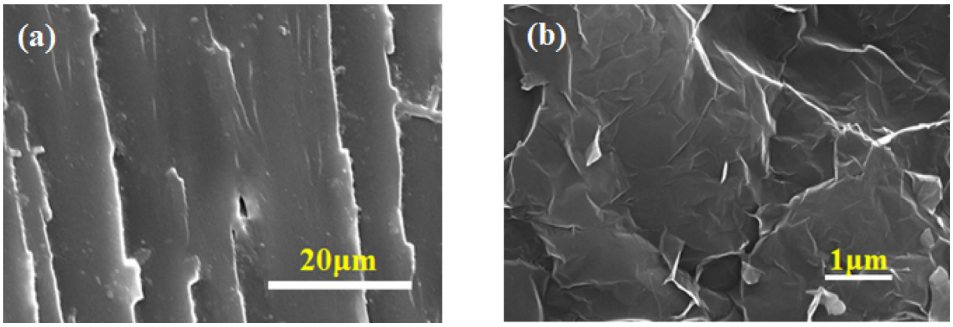


**Fig. 2.** SEM micrograph of (a) prinstine epoxy (b) dispersion of graphene with epoxy matrix.

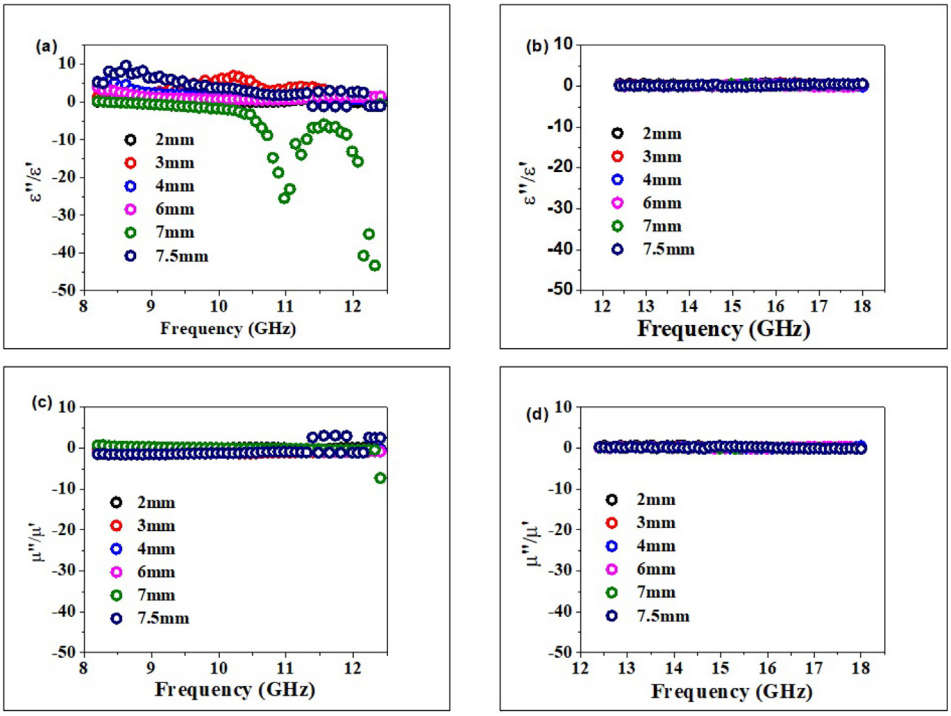


**Fig. 3.** (a) Dielectric loss for various thickness at X-band (b)) Dielectric loss for various thickness at Ku-band (c) Magnetic loss for various thickness at X-band (d) Magnetic loss for various thickness at Ku-band.

### *3.4. EMI shielding effectiveness*

The reflection loss, absorption loss and shielding effectiveness were studied for various thickness of GrEpCoF composites. Those samples were tested under the spectrum of two bands, viz. X and Ku. The losses were calculated from S-parameters $S_{11}$ and $S_{21}$ following (1)–(3). Fig. 4 (a-f) shows the variation of the total SE, reflection, and absorption losses with thickness for both the bands under consideration.

The reflection loss were calculated by,

$$SE_R = 10\log 10^{\frac{S11}{10}} \quad (1)$$

The total shield effectiveness were calculated by,

$$SE_T = S_{21} \quad (2)$$

The absorption loss were caculated by,

$$SE_A = SE_T - SE_R \quad (3)$$

The maximum reflection loss was obtained for the composite with 2 mm thickness as can be depicted from Fig. 4 (a). Further, increase in the thickness of composite results in the decrease of the reflection loss value. However, in the case of absorption loss, losses are seen to increases with thickness, Fig. 4 (b). The total shielding effectiveness also showed an improvement with thickness. The composite with a thickness of 2 mm showed $SE_T$ in the range of −4 dB, whereas for the samples with the maximum thickness of 7 and 7.5 mm $SE_T$ values of approximately −12 dB was obtained. Fig. 4(c) show that the 7 mm composite exhibit the maximum shielding efficiency, which is around −14 dB. In it also worth noting that in samples with thickness 7 and 7.5 mm, the bandwidth included the entire X-band.

In contrast to X-band, the reflection loss of Ku-band was negligible and was independent of thickness for GrEpCoF composite material as shown in Fig. 4(d). However, in contrast to reflection loss, the samples exhibited a greater absorption loss. The values of obtained absorption loss was higher than in the case of X-band. A clear increase in absorption loss with thickness is noticeable from Fig. 4(e). The maximum absorption loss was exhibited by the composite of 7 mm thickness. Due to the negligible effect of reflection loss, the total shielding effectiveness is mainly due to absorption loss. This is extremely useful in practical applications as the reflected EM waves can lead to secondary absorption [16]. A

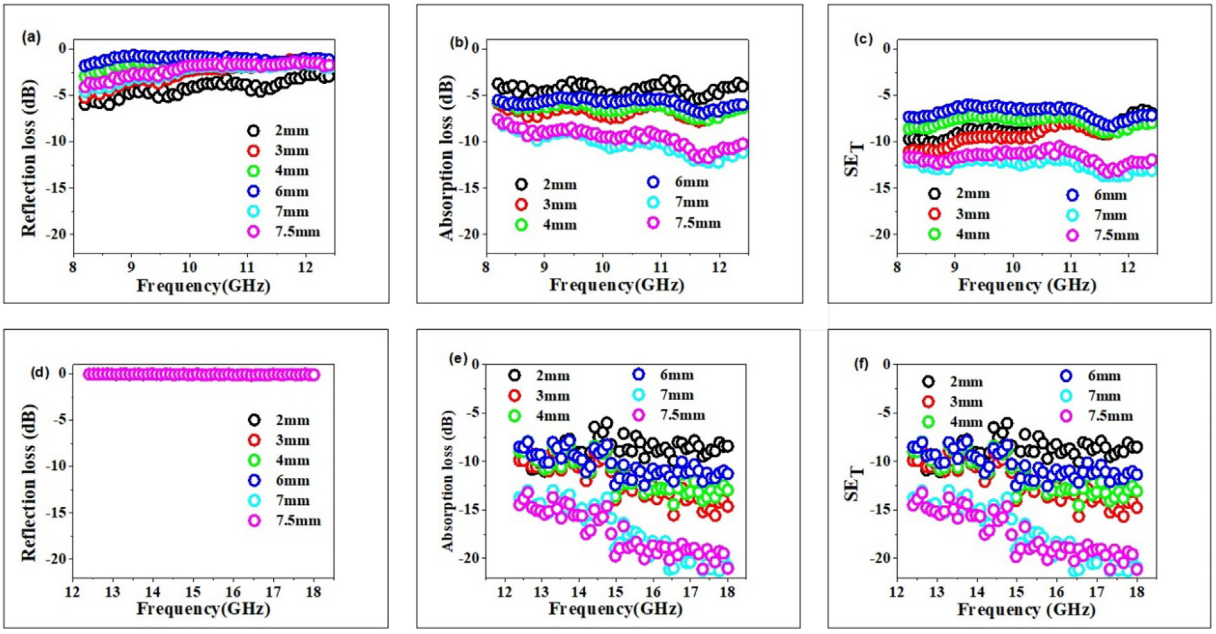


**Fig. 4.** (a) The variation in Reflection loss with frequency in X band, (b) The variation in absorption loss with frequency loss and (c) Total shield effectiveness for X-band with various thickness of composite films; (d) The variation in Reflection loss with frequency in Ku band, (e) The variation in absorption loss with frequency loss and (f) Total shield effectiveness for Ku-band with various thickness of GrEpCoF composite films.

maximum $SE_T$ of –22 dB was observed in Ku-band. It is also worth noting that for samples with 7 mm and 7.5 mm thickness, $SE_T$ is below – 10 dB for the entire Ku-band, showing that these samples exhibit a band width of 10 GHz (from 8.2 to 18 GHz). This shows that the composite samples containing 5 wt% CoF, 1 wt% Gr and rest epoxy is able to shield 90% of the microwave radiations in the range of 8.2 to 18 GHz. The enhancement in $SE_T$ in spite of the poor dielectric and magnetic loss could be attributed to the other loss mechanisms such as interfacial polarization, natural resonance, and multiple scatterings due to the additives and multiple reflections leading to a longer path for the waves, thereby enhancing absorption [17].

## 4. Conclusion

The effect of thickness of Epoxy/Gr/CoF composite samples on dielectric loss, magnetic loss, and EMI shielding effectiveness ($SE_T$) are reported. Due to the low amount of CoF, the samples had a very low dielectric loss and a very low magnetic loss. In spite of this, a high value of $SE_T$ (up to –22 dB) was exhibited by samples with 7 mm and 7.5 mm thickness with a bandwidth spanning the entire X-band and Ku-band. It is worth noting that reflection loss is higher for lower frequencies and becomes less relevant at higher frequencies. Reflection loss is also prominent for thinner samples and decreases with increased thickness. The absorption loss, on the other hand, is the opposite and is found to increase with frequency. With increasing sample thickness, it is seen that losses are increasing. Further studies are required using a higher concentration of CoF and Gr to achieve a better $SE_T$ value.

## CRediT authorship contribution statement

**S. Manobalan:** Methodology, Investigation, Writing – original draft. **Suryasarathi Bose:** Resources. **T.P. Sumangala:** Conceptualization, Writing – review & editing, Supervision.

## Data availability

Data will be made available on request.

## Declaration of Competing Interest

The authors declare that they have no known competing financial interests or personal relationships that could have appeared to influence the work reported in this paper.

## Acknowledgement

The authors thank Vellore Institute of Technology, Vellore for providing 'VIT SEED Grant - RGEMS fund (SG20220118) for carrying out this research work.

## References

[1] B. Steinfeld, J. Scott, G. Vilander, L. Marx, M. Quirk, J. Lindberg, K. Koerner, The role of lean process improvement in implementation of evidence-based practices in behavioral health care, J. Behav. Heal. Serv. Res. 42 (4) (2015) 504–518.
[2] B. Anasori, M.R. Lukatskaya, Y. Gogotsi, 2D metal carbides and nitrides (MXenes) for energy storage, Nat. Rev. Mater. 2 (2) (2017) 1–17.
[3] J.M. Thomassin, C. Jerome, T. Pardoen, C. Bailly, I. Huynen, C. Detrembleur, Polymer/carbon based composites as electromagnetic interference (EMI) shielding materials, Mater. Sci. Eng. R. Rep. 74 (7) (2013) 211–232.
[4] Y. Zhang, Y. Yan, H. Qiu, Z. Ma, K. Ruan, J. Gu, A mini-review of MXene porous films: preparation, mechanism and application, J. Mater. Sci. Technol. 103 (2022) 42–49.
[5] R. Sun, H.B. Zhang, J. Liu, X. Xie, R. Yang, Y. Li, et al., Highly conductive transition metal carbide/carbonitride (MXene)@ polystyrene nanocomposites fabricated by electrostatic assembly for highly efficient electromagnetic interference shielding, Adv. Funct. Mater. 27 (45) (2017) 1702807.
[6] Y. Han, K. Ruan, J. Gu, Janus (BNNS/ANF)-(AgNWs/ANF) thermal conductivity composite films with superior electromagnetic interference shielding and Joule heating performances, Nano Res. 15 (5) (2022) 4747–4755.
[7] J. Gao, J. Luo, L. Wang, X. Huang, H. Wang, X. Song, H. Xue, Flexible, superhydrophobic and highly conductive composite based on non-woven polypropylene fabric for electromagnetic interference shielding, Chem. Eng. J. 364 (2019) 493–502.
[8] C. Liang, M. Hamidinejad, L. Ma, Z. Wang, C.B. Park, Lightweight and flexible graphene/SiC-nanowires/poly (vinylidene fluoride) composites for

electromagnetic interference shielding and thermal management, Carbon 156 (2020) 58–66.
[9] L. Wang, Z. Ma, Y. Zhang, L. Chen, D. Cao, J. Gu, Polymer-based EMI shielding composites with 3D conductive networks: a mini-review, SusMat 1 (3) (2021) 413–431.
[10] A.K. Singh, A. Shishkin, T. Koppel, N. Gupta, A review of porous lightweight composite materials for electromagnetic interference shielding, Compos. B Eng. 149 (2018) 188–197.
[11] S. Manobalan, C. Mahender, D. Rajan Babu, A. Rahaman, M.S. Sreekanth, D. Sharma, et al., The Mechanical, Dielectric, and EMI Shielding Properties of Nickel Ferrite (NiF)/Graphene (Gr)-Doped Epoxy Composites, J. Inorg. Organomet. Polym Mater. 32 (10) (2022) 4077–4091.
[12] P. Xiong, Q. Chen, M. He, X. Sun, X. Wang, Cobalt ferrite–polyaniline heteroarchitecture: a magnetically recyclable photocatalyst with highly enhanced performances, J. Mater. Chem. 22 (34) (2012) 17485–17493.
[13] E.E. Tanrıverdi, A.T. Uzumcu, H. Kavas, A. Demir, A. Baykal, Conductivity study of polyaniline-cobalt ferrite (PANI-CoFe2O4) nanocomposite, Nano-Micro Letters 3 (2) (2011) 99–107.
[14] N.E. Kazantseva, Y.I. Bespyatykh, I. Sapurina, J. Stejskal, J. Vilčáková, P. Sáha, Magnetic materials based on manganese–zinc ferrite with surface-organized polyaniline coating, J. Magn. Magn. Mater. 301 (1) (2006) 155–165.
[15] Ö. Yavuz, M.K. Ram, M. Aldissi, P. Poddar, S. Hariharan, Synthesis and the physical properties of MnZn ferrite and NiMnZn ferrite–polyaniline nanocomposite particles, J. Mater. Chem. 15 (7) (2005) 810–817.
[16] C. Liang, P. Song, H. Qiu, Y. Huangfu, Y. Lu, L. Wang, J. Kong, J. Gu, Superior electromagnetic interference shielding performances of epoxy composites by introducing highly aligned reduced graphene oxide films, Compos. A Appl. Sci. Manuf. 124 (2019).
[17] M. Verma, A.P. Singh, P. Sambyal, B.P. Singh, S.K. Dhawan, V. Choudhary, Barium ferrite decorated reduced graphene oxide nanocomposite for effective electromagnetic interference shielding, Phys. Chem. Chem. Phys. 17 (2015) 1610–1618.